NAVAL POSTGRADUATE SCHOOL

MONTEREY, CALIFORNIA

THESIS

INVESTIGATION OF ACOUSTIC CHARACTERISTICS AND DB REDUCTION OF MICROSPHERE-BASED PANELING ON DIVING WETSUITS

by

Jared H. Young

June 2021

Thesis Advisor: Emil P. Kartalov
Second Reader: Bruce C. Denardo

THIS PAGE INTENTIONALLY LEFT BLANK

REPORT DOCUMENTATION PAGE			*Form Approved OMB No. 0704-0188*

1. AGENCY USE ONLY *(Leave blank)*	**2. REPORT DATE** June 2021	**3. REPORT TYPE AND DATES COVERED** Master's thesis

4. TITLE AND SUBTITLE INVESTIGATION OF ACOUSTIC CHARACTERISTICS AND DB REDUCTION OF MICROSPHERE-BASED PANELING ON DIVING WETSUITS	**5. FUNDING NUMBERS**
6. AUTHOR(S) Jared H. Young	
7. PERFORMING ORGANIZATION NAME(S) AND ADDRESS(ES) Naval Postgraduate School Monterey, CA 93943-5000	**8. PERFORMING ORGANIZATION REPORT NUMBER**
9. SPONSORING / MONITORING AGENCY NAME(S) AND ADDRESS(ES) N/A	**10. SPONSORING / MONITORING AGENCY REPORT NUMBER**

11. SUPPLEMENTARY NOTES The views expressed in this thesis are those of the author and do not reflect the official policy or position of the Department of Defense or the U.S. Government.

12a. DISTRIBUTION / AVAILABILITY STATEMENT Approved for public release. Distribution is unlimited.	**12b. DISTRIBUTION CODE** A

13. ABSTRACT (maximum 200 words)

Scuba divers are exposed to potentially harmful temperatures and noise intensities while operating underwater. Standard neoprene wetsuits modified with glass-microsphere composite panels have been shown to improve the thermal capabilities of the suit and retain more of the diver's body heat. While neoprene is an effective sound absorber itself, the acoustic properties and sound-proofing capabilities of the created composite panels were investigated. Several composite panels were used to shield a hydrophone receiver from a source signal over a range of frequencies from 10 Hz to 20 kHz and compared to a 7 mm neoprene sample. Results indicate a variable dB reduction in sound pressure over this range, with the measured intensity transmission coefficients of the composites being comparable to neoprene past a frequency of approximately 13 kHz. When used in tandem with neoprene, the material further reduces the measured pressure of the source signal. While not as effective as neoprene itself, the composite material shows potential for underwater soundproofing uses. Further experimentation with panel composition may yield a more effective sound absorbing material.

14. SUBJECT TERMS diver, wetsuit, frequency response, acoustic transmission	**15. NUMBER OF PAGES** 67
	16. PRICE CODE

17. SECURITY CLASSIFICATION OF REPORT	**18. SECURITY CLASSIFICATION OF THIS PAGE**	**19. SECURITY CLASSIFICATION OF ABSTRACT**	**20. LIMITATION OF ABSTRACT**
Unclassified	Unclassified	Unclassified	UU

NSN 7540-01-280-5500

Standard Form 298 (Rev. 2-89)
Prescribed by ANSI Std. 239-18

THIS PAGE INTENTIONALLY LEFT BLANK

Approved for public release. Distribution is unlimited.

INVESTIGATION OF ACOUSTIC CHARACTERISTICS AND DB REDUCTION OF MICROSPHERE-BASED PANELING ON DIVING WETSUITS

Jared H. Young
Ensign, United States Navy
BS, U.S. Naval Academy, 2020

Submitted in partial fulfillment of the
requirements for the degree of

MASTER OF SCIENCE IN ENGINEERING ACOUSTICS

from the

NAVAL POSTGRADUATE SCHOOL
June 2021

Approved by: Emil P. Kartalov
Advisor

Bruce C. Denardo
Second Reader

Oleg A. Godin
Chair, Department of Physics

THIS PAGE INTENTIONALLY LEFT BLANK

ABSTRACT

Scuba divers are exposed to potentially harmful temperatures and noise intensities while operating underwater. Standard neoprene wetsuits modified with glass-microsphere composite panels have been shown to improve the thermal capabilities of the suit and retain more of the diver's body heat. While neoprene is an effective sound absorber itself, the acoustic properties and sound-proofing capabilities of the created composite panels were investigated. Several composite panels were used to shield a hydrophone receiver from a source signal over a range of frequencies from 10 Hz to 20 kHz and compared to a 7 mm neoprene sample. Results indicate a variable dB reduction in sound pressure over this range, with the measured intensity transmission coefficients of the composites being comparable to neoprene past a frequency of approximately 13 kHz. When used in tandem with neoprene, the material further reduces the measured pressure of the source signal. While not as effective as neoprene itself, the composite material shows potential for underwater soundproofing uses. Further experimentation with panel composition may yield a more effective sound absorbing material.

THIS PAGE INTENTIONALLY LEFT BLANK

TABLE OF CONTENTS

I. INTRODUCTION....1
A. BACKGROUND....1
B. PREVIOUS WORK....2
C. ACOUSTIC BACKGROUND....2
D. PANEL FABRICATION....7
E. WETSUIT CONSTRUCTION....14

II. INVESTIGATION OF ACOUSTIC CHARACTERISTICS....17
A. ACOUSTIC THEORY....17
B. BASIC FREQUENCY RESPONSE MODELS....20

III. EXPERIMENTAL SETUP....25

IV. RESULTS AND ANALYSIS....29
A. FREQUENCY RESPONSE....29
B. PRESSURE REDUCTION....30
C. TRANSMISSION....34
D. CERAMIC MICROSPHERES....35
E. MATERIAL COMPARISON....41

V. CONCLUSION....43

LIST OF REFERENCES....45

INITIAL DISTRIBUTION LIST....47

THIS PAGE INTENTIONALLY LEFT BLANK

LIST OF FIGURES

Figure 1. Preliminary dive test showing improved heat retention within the K-Suit Mk. I compared to a standard 7 mm wetsuit. Adapted from [1]. 2

Figure 2. Human hearing threshold with and without diving equipment. Source: [4].....4

Figure 3. 3D body scans were translated into SolidWorks to create two-piece molds for the casting process. Source: [6]. 8

Figure 4. K1 glass microspheres were added to the 10:1 ratio of elastomer base and curing agent; approximately 150 mL of these microspheres were used in each cup 9

Figure 5. Composite mixtures were placed in a THINKY planetary rotary mixer for 4 min at 1500 rpm to allow for thorough mixing.....10

Figure 6. Composite mixtures were degassed and poured into the lower section of the printed mold 11

Figure 7. Sealed molds were placed into the VWR Forced Air Oven at 80°C for 2 hours 12

Figure 8. After curing, the top portion of the mold was removed, and the completed panel was extracted 13

Figure 9. Excess material from the edges and mold shafts were trimmed from the extracted panel 13

Figure 10. Several completed composite panels trimmed and labeled before being attached to the wetsuit.....14

Figure 11. Completed K-suit Mk. II with glass microsphere-based composite panels 15

Figure 12. Transmission of normal incidence sound signal on a fluid layer. Adapted from [7].....17

Figure 13. Plot of the left-hand cutoff inequality (black) for the 3-component approximation. Note that it never approaches a magnitude near 1 to satisfy the inequality 21

Figure 14. Estimated transmission curves for the two-component approximation using silicone elastomer and glass (neglecting air).....22

Figure 15. Estimated transmission curves for simplistic glass model (neglecting air and silicone elastomer base) 23

Figure 16. O5 and O10 composite pucks constructed with glass microspheres 25

Figure 17. Hydrophone and composite puck arrangement behind neoprene material (held out of tank for visualization) 27

Figure 18. A gated FFT sweep was conducted to verify that no sound echoes/ reflections were present. Ch.1 (Yellow) shows the speaker chirp, while Ch.2 (Blue) is the hydrophone recording....28

Figure 19. Raw captured data showing frequency response for the tested materials in units of pressure (converted from captured dB re V/μPa) 29

Figure 20. Ratio of measured pressure behind material shielding and hydrophone baseline 31

Figure 21. Ratio of measured pressure behind O5 and O10 pucks and hydrophone baseline 32

Figure 22. Ratio between measured material pressure and hydrophone baseline in dB....33

Figure 23. Ratio between measured O5 and O10 pressure and hydrophone baseline in dB....34

Figure 24. Pressure transmission coefficients for all tested materials relative to hydrophone baseline 35

Figure 25. Pressure transmission coefficients for composite material pucks relative to hydrophone baseline 35

Figure 26. Ceramic frequency response of C20 and C50 material pucks 36

Figure 27. Ratio of measured pressure behind ceramic material shielding and hydrophone baseline 37

Figure 28. Ratio of measured pressure behind C20 and C50 pucks and hydrophone baseline 38

Figure 29. Ratio between measured ceramic material pressure and hydrophone baseline in dB....39

Figure 30. Ratio between measured C20 and C50 pressure and hydrophone baseline in dB....40

Figure 31. Pressure transmission coefficients for all tested ceramic materials relative to hydrophone baseline 41

Figure 32. Pressure transmission coefficients for ceramic material pucks relative to hydrophone baseline 41

THIS PAGE INTENTIONALLY LEFT BLANK

LIST OF TABLES

Table 1. Bio-effects of low-frequency underwater sound (100-500 Hz). Source: [4].....6

Table 2. Bio-effects of underwater sound (500-2500 Hz). Source: [4]. 6

Table 3. Tabulated values for approximation of sound speed 20

THIS PAGE INTENTIONALLY LEFT BLANK

LIST OF ACRONYMS AND ABBREVIATIONS

dB	decibel
°F	degrees Fahrenheit
DOD	Department of Defense
FFT	Fast Fourier Transform
IL	Intensity Level
LFS	Low Frequency Sonar
Pa	Pascal
PDMS	polydimethylsiloxane
SPL	Sound Pressure Level
SRS	Stanford Research Systems

THIS PAGE INTENTIONALLY LEFT BLANK

ACKNOWLEDGMENTS

I would like to thank both the U.S. Navy and the Naval Postgraduate School for their support on this thesis. Advice and direction from my advisor, Dr. Emil Kartalov, as well as Dr. Oleg Godin and Dr. Bruce Denardo were invaluable in preparing the experimentation and analyzing the data presented in this thesis. I would also like to thank Jay Adeff for his help preparing the test equipment in the tank lab. Finally, the suit could not have been made without Otter Bay Wetsuits in Monterey.

THIS PAGE INTENTIONALLY LEFT BLANK

I. INTRODUCTION

A. BACKGROUND

Scuba diving is an extremely popular activity, allowing people to explore an entirely different world beneath the surface of the water. Many dive simply for recreation or sport, while others dive commercially in the field of salvage and recovery or while conducting military operations. While common, diving is not without its dangers, as divers are presented with a limited supply of breathable oxygen and are often exposed to fairly extreme temperatures, especially at great depths. Even warm water can produce hypothermic conditions, which occur when the core body temperature falls below 95°F [1]. This risk is reduced by wearing wetsuits made of neoprene material.

Neoprene is an effective insulator of body heat due to air bubbles trapped in it, as it contains this heat within the wetsuit. Water within the suit is warmed by the body itself, and any water flow in and out of the suit should be minimized to mitigate heat transfer. As pressure increases as a diver descends in the water, however, the neoprene compresses and loses much of its thermal insulation.

Neoprene is also an extremely effective sound absorber due to its porous nature. Porous materials are generally the best sound absorbers, as the air/gas molecules contained within them interact via friction to dissipate energy as heat. Conversely, non-porous materials lack this ability to dissipate energy to the same effect. It is also known that pairing non-porous materials with a porous material acts to reduce the dissipation effect [2]. Therefore, it would be expected for neoprene to serve as a widely used soundproofing material. Regrettably, neoprene is extremely toxic when it breaks down, producing gases such as chlorine, formaldehyde, lead, and hydrochloric acid. This has resulted in the material becoming red-listed, which is a label given to materials known to pose severe health risks to both humans and the environment. While neoprene is very effective, alternatives should be found that can be utilized safely over time.

B. PREVIOUS WORK

The precursor to this study saw LT Shane Martin investigate the thermal properties of a wetsuit supplemented with glass microsphere-based panels, dubbed the "K-Suit Mk. 1." These panels were constructed using 3M K1 glass microspheres embedded in a hardened elastomer (similarly presented in this thesis), with a thermal conductivity of 0.047 $W/(m * K)$ and a pressure tolerance of about 500 feet [1]. The constructed panels were added to a standard neoprene wetsuit and temperature readings were collected over several dives. The results of one of these dives is shown in Figure 1.

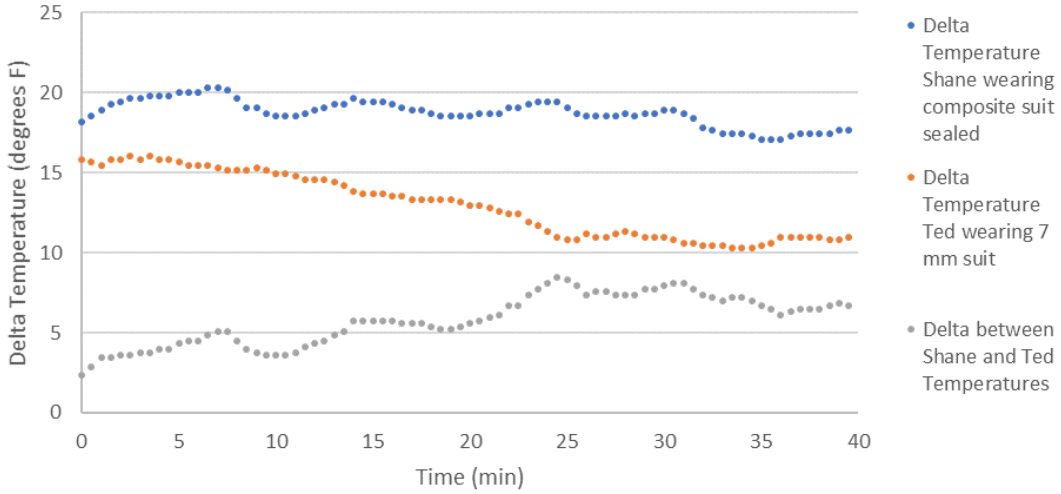

Figure 1. Preliminary dive test showing improved heat retention within the K-Suit Mk. I compared to a standard 7 mm wetsuit. Adapted from [1].

LT Martin's data shows a clear improvement in thermal insulation over standard neoprene. A concurrent project is improving on the Mk. I suit (by adding thermal protection for the upper/lower arms and lower legs) and further investigating the thermal insulation of the K-Suit Mk. II.

C. ACOUSTIC BACKGROUND

Wetsuits are often supplemented with neoprene dive hoods, which further increase the thermal protection around the diver's head. Hoods also have the ability to insulate the

diver from loud underwater sounds due to the sound-proofing characteristics of neoprene. Underwater sound itself is a result of vibrations and pressure fluctuations in the water. The compressional nature of sound waves means that sounds underwater travel much faster than they otherwise would in air. This is due to an increased ratio between the stiffness and inertia of the water when compared to that of air. Because of this, energy is transferred at a greater rate through the water, yielding a louder sound than what would be received in air.

A sound's "loudness" is generally established by its amplitude and is related to sound pressure and sound power. Sound power is most commonly measured via intensity, which is defined as the ratio of acoustic power to area ($\mathrm{W/m^2}$), or as pressure, which is the force per unit area of a sound on a surface (Pa). Both of these measurements can be expressed on the logarithmic decibel (dB) scale as Intensity Level (IL) and Sound Pressure Level (SPL), respectively.

$$IL = 10\,log_{10}\frac{I}{I_{ref}} \tag{1}$$

$$SPL = 20\,log_{10}\frac{p_{rms}}{p_{ref}} \tag{2}$$

Note that these formulae are different but mutually consistent, as intensity and power are related by the square of the amplitude or pressure. As defined, the above ensure direct equality of the levels regardless of the calculation being based on pressure/amplitude or power/intensity.

Previous studies have determined safe exposure limits for divers at various SPLs, as well as created distance and exposure time reference sheets for military use [3]; these references show that hooded divers can tolerate higher SPLs and do so for slightly longer periods of time. A military diver's exposure limits become extremely important when faced with modernized diver deterrence techniques, such as swimmer neutralization equipment or active sonar systems. It is possible that adding additional shielding to a wetsuit and hood can increase the provided sound proofing effect, enabling higher exposure tolerances. As fabrication for the K-suit Mk. II was underway to further investigate its thermal properties,

testing could be carried out on the microsphere panel's acoustic properties and determine their effectiveness in reducing transmitted sound intensity.

For soundproofing in diving applications, it is important to reference the human hearing threshold, which is between about 20 Hz and 11 kHz in air. This range is about the same underwater during bareheaded diving (without a hood or helmet). Adding a hood and full-face mask reduces this threshold to between 110 Hz and 1300 Hz [4]. Figure 2 presents these auditory thresholds with the addition of and absence of standard diving headgear. Note that the SPL values are the lowest discernable value.

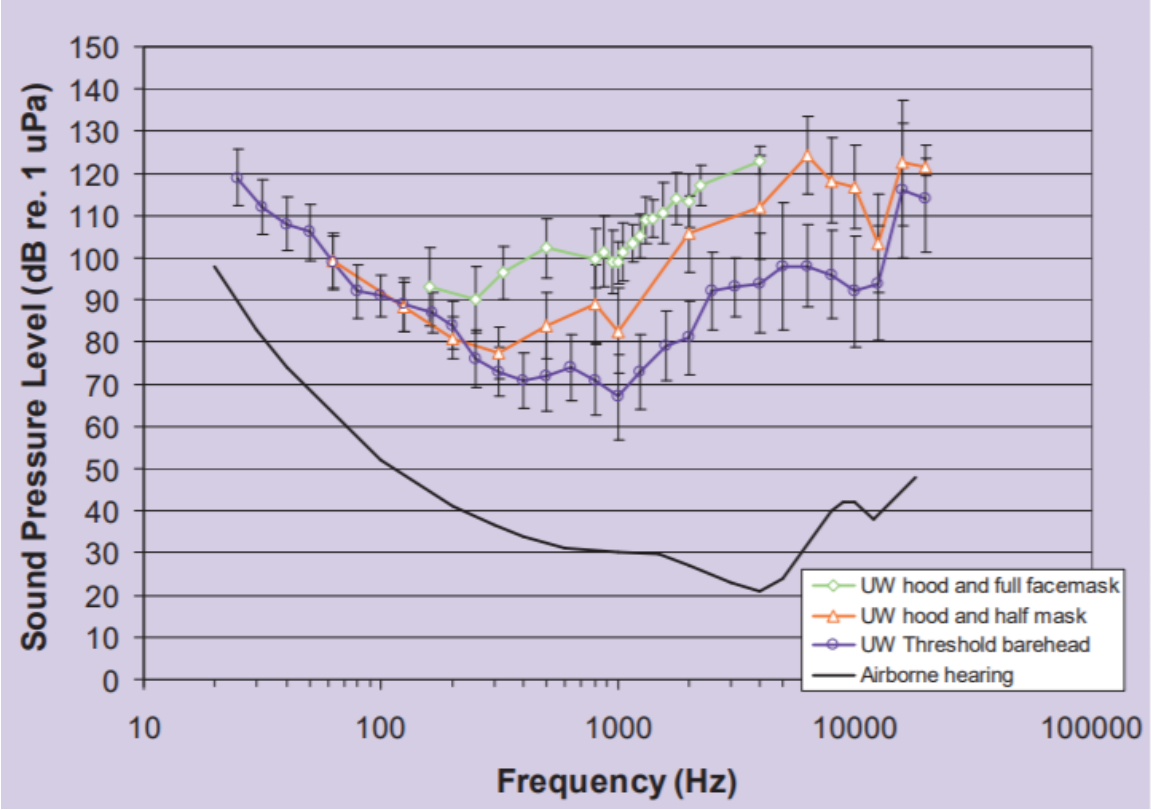

Figure 2. Human hearing threshold with and without diving equipment. Source: [4].

Interestingly, different frequency bands impact the human body in different ways. Different frequency bands have been seen to produce various symptoms within human divers known as 'bioeffects'. Several branches of the Department of Defense (DOD) have

investigated such bioeffects, with study results being used to implement diver-neutralization techniques [5]. As stated in an ARL: UT report on this topic, "acoustic energy, applied at specific frequencies, amplitudes, and durations […] would affect the function and/or physical characteristics of major organs, limbs, or central nervous system in a measurable manner" [5]. These bioeffects, for example, can range from marginal discomfort to full auditory damage and tissue trauma.

Low Frequency Sonar (LFS) (100 – 500 Hz) generates high-energy pulses of sound which may be harmful at high power levels. High intensity LFS most commonly results in non-auditory effects, such as vertigo and dizziness, tingling, chest/lung tissue resonance effects, and muscle contractions within the body [5]. While these effects are not necessarily fatal, the resultant discomfort will very likely cause the diver to abandon an operation or return to the surface. Navy testing determined safe operating limits, outlining a recommendation at 160 – 320 Hz with a maximum SPL of 160 dB re 1 μPa for no more than 100 seconds [5]. Human testing saw physical aversion begin in divers within the LFS range at an SPL exceeding 140 dB, with most divers reporting a 'very severe' aversion level at the 100 Hz frequency. A summary of bioeffects from this study is show in Table 1 for the lower frequencies of 100 to 500 Hz and Table 2 for the range of 500 to 2500 Hz. It should also be noted that Navy regulations prohibit diver exposure at an SPL exceeding 215 dB, regardless of frequency or equipment used.

Table 1. Bio-effects of low-frequency underwater sound (100-500 Hz). Source: [4].

SPL dB re.1 µPa	Effect 100 to 500 Hz
184 +	Based on animal models liver haemorrhage and soft tissue damage are likely.
170+	Tolerance limit for divers and swimmers. Sound causes lung and body vibration.
148 -157	The loudness and vibration levels become increasingly aversive. Some divers will contemplate aborting an open water dive.
140 -148	A small number of divers rate the sound as 'very severe'.
136 -140	The sound is clearly audible. The majority of divers tolerate the sound well with only "Slight" aversion.
130	Divers and swimmers able to detect body vibration
80 -100	Auditory Threshold

Table 2. Bio-effects of underwater sound (500-2500 Hz). Source: [4].

SPL dB re.1 µPa	Effect 500 to 2500 Hz
190 +	Hooded diver tolerance limit
167 - 185	Tolerance limit for barehead divers and swimmers. Sound causes dizziness and disorientation. Divers in suit and hood are able to tolerate the sound well.
155 - 166	Divers tolerate these sounds well, although an increasing number of bareheaded divers indicate a 'severe' aversion rating.
140 - 154	Sound is clearly audible to divers. Sound is tolerated well with only slight aversion.
100 - 140	Divers hear underwater sound, but it is masked by exhaust bubble noise.
80	Hearing threshold for hooded divers
65	Hearing threshold for barehead divers

Higher frequencies also produce varying impacts; In many cases, exposure above this LFS range resulted in auditory discomfort in divers between 500 and 2500 Hz. Certain frequencies are also seen to illicit dizziness and impact balance at SPLs above 150 dB [4]. While much of this discomfort comes in the form of excessive loudness, there are studies that suggest resonance with internal organs [5]. Even higher frequencies in the Ultrasonic band (1-4 MHz) produce cavitation (bubble formation) and heating effects upon exposure. Tissue damage is known to occur if exposure is too long and at close enough ranges. Bubble formation is dependent on SPL and frequency, with bubbles beginning to collapse at high enough pressures and releasing energy upon compression. U.S. Navy studies have determined exposure ranges based on these effects, stating that a diver may not be closer than 10 yards when operating near a sound source exceeding 250 kHz [5]. It should be noted, however, that power generated by ultrasonic signals is dissipated rapidly with distance, as well as that frequencies below 100 kHz produced negligible heating effects.

D. PANEL FABRICATION

The previous study conducted with the K-suit Mk. I generated 3D body scans of the divers wearing a thin neoprene wetsuit. These scans were modified in SolidWorks and used to produce various rectangular molds (Figure 3), allowing for the casting of individual panels. Molds were printed in two components in polycarbonate on a Fortis mc400 3D printer using a half-density mesh setting. The mold lid was printed with several empty shafts to allow air to vent and excess material to escape if overfilled. The lid was also printed about 5% smaller in scale than the associated base. This gap allowed for a slightly thicker panel to be constructed.

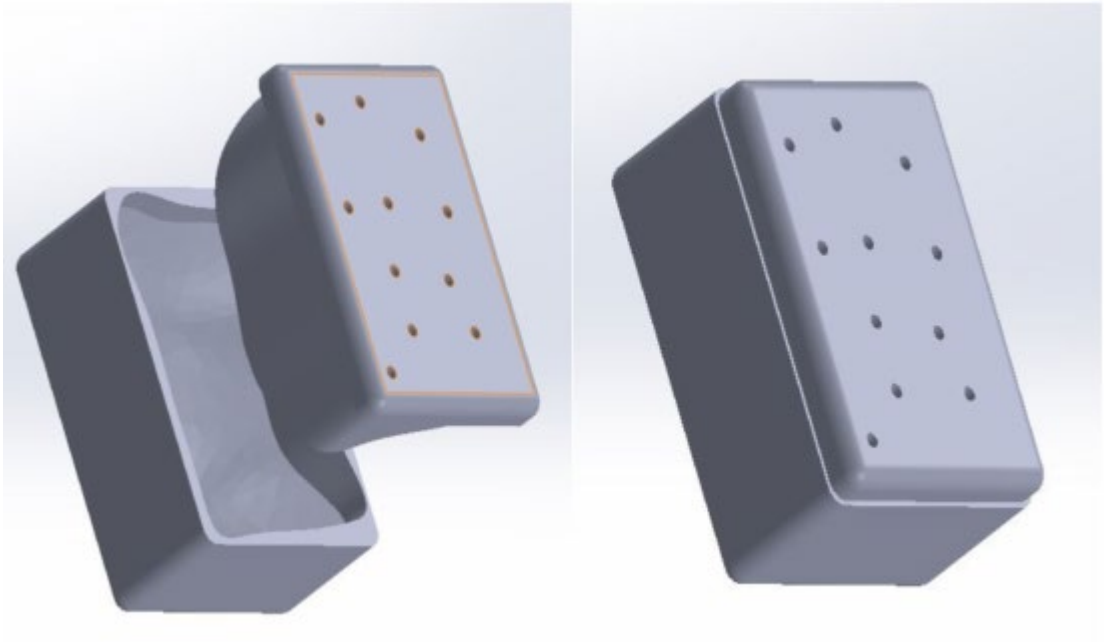

Figure 3. 3D body scans were translated into SolidWorks to create two-piece molds for the casting process. Source: [6].

The silicone prepolymer for the wetsuit panels was created by mixing a 10:1 ratio of Dow Corning Corp. Sylgard 184 polydimethylsiloxane (PDMS) silicone elastomer base and curing agent. Approximately 100g of the elastomer base was mixed with ~10g of the curing agent in a 310 mL mixing cup before adding ~150 mL of 3M K1 hollow glass microspheres. Space was deliberately left in the cup to allow for a thorough mixing to occur. Figure 4 shows the addition of the K1 microspheres to a mixing cup holding the elastomer base and curing agent.

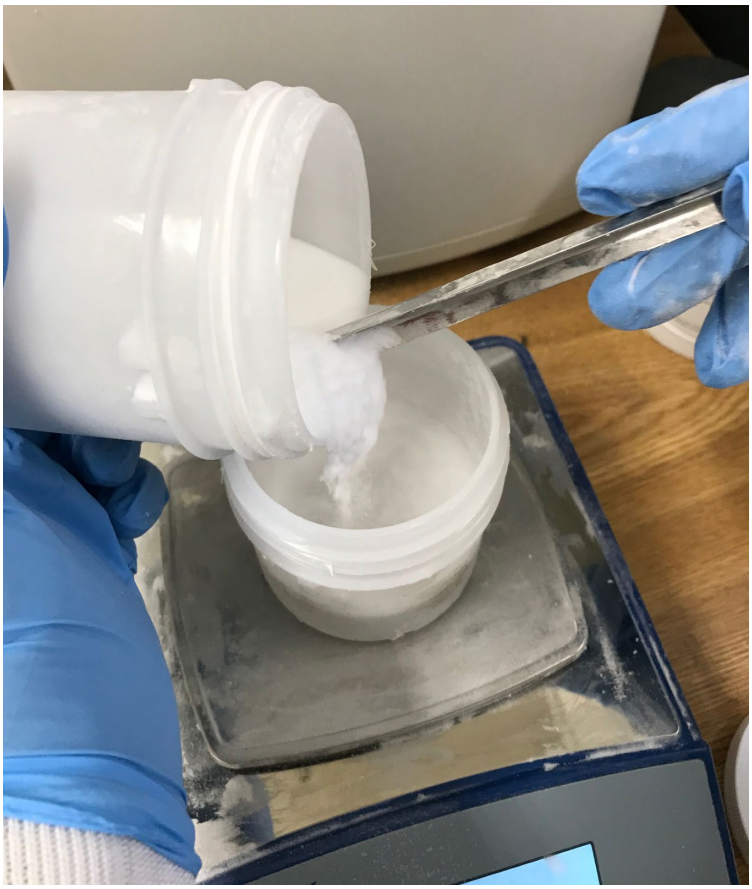

Figure 4. K1 glass microspheres were added to the 10:1 ratio of elastomer base and curing agent; approximately 150 mL of these microspheres were used in each cup

The mixing cup was sealed and spun at 1500 rpm for 4 min in an ARE-310 THINKY planetary rotary mixer. This method allowed for a bladeless mixing of the material to avoid damage to the embedded microspheres. As seen in Figure 5, the mixing cup is held at an angle within the mixer to create a three-dimensional flow of material. A counterweight within the mixer, opposite to the cup, was also set to balance the centrifugal force of the cup.

Figure 5. Composite mixtures were placed in a THINKY planetary rotary mixer for 4 min at 1500 rpm to allow for thorough mixing

Multiple cups were prepared for each mold (two to four depending on size) and were placed in a desiccator attached to a mechanical vacuum pump. Mixtures were degassed for approximately 5 min before being poured into the bottom section of the prepared molds; Figure 6 Shows two cups being poured into one such mold.

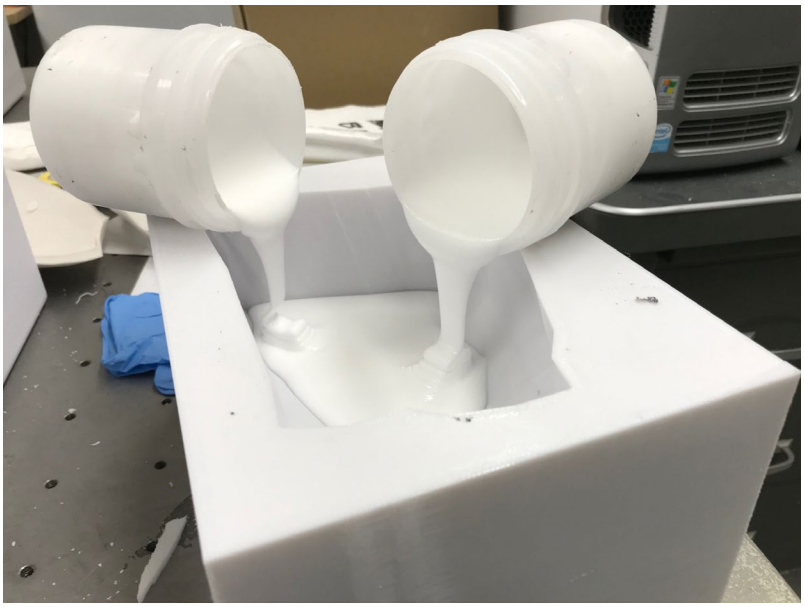

Figure 6. Composite mixtures were degassed and poured into the lower section of the printed mold

The lid was pressed firmly into the lower mold section before the being placed into a VWR Forced Air Oven at 80℃ for 2 hours. for faster material curing (Figure 7); standard material cure time is 24 hours. at room temperature.

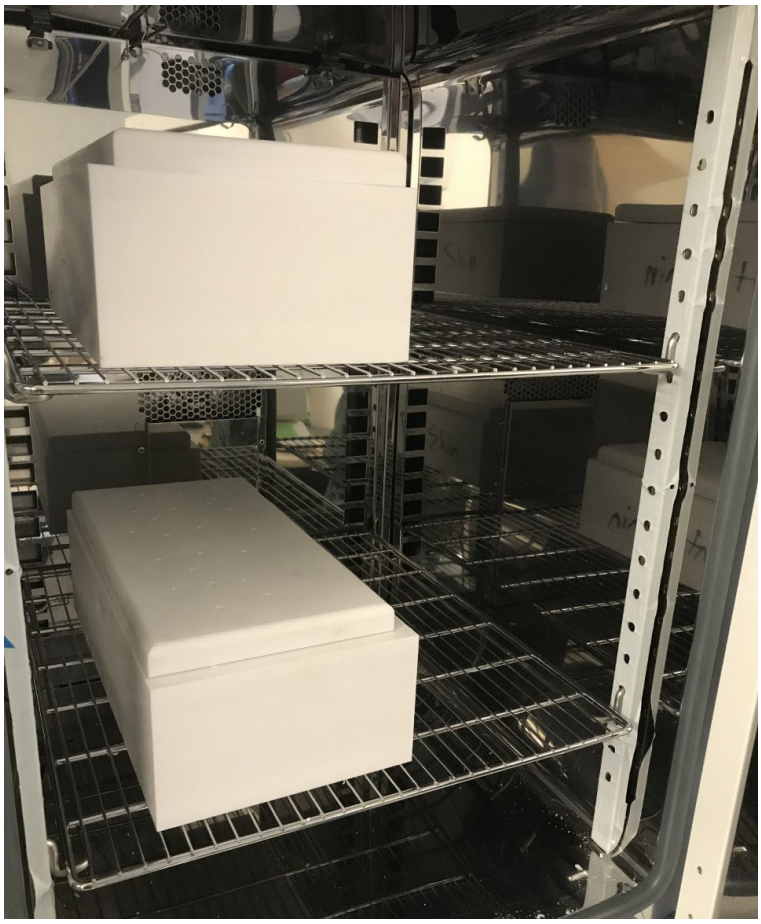

Figure 7. Sealed molds were placed into the VWR Forced Air Oven at 80℃ for 2 hours

The mold was removed from the oven and cooled to room temperature. The cast was extracted, and excess debris was removed from the molds before the next iteration of panels were created. Vent shafts on the molds were drilled to clear any residual obstruction from excess material. Any excess material on the cast itself was trimmed with a razor and discarded (figures 8 and 9).

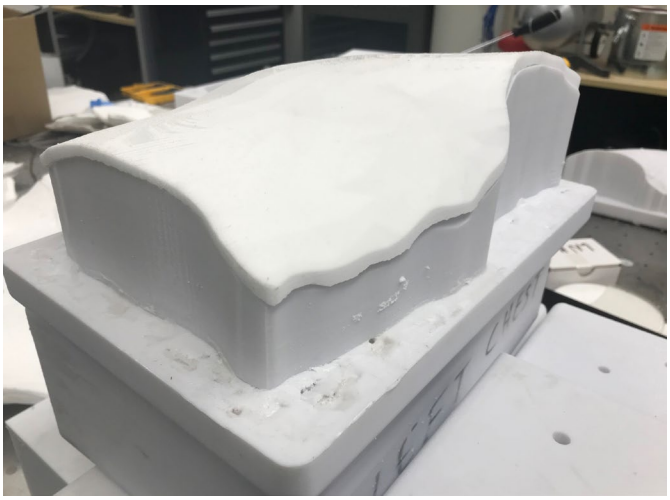

Figure 8. After curing, the top portion of the mold was removed, and the completed panel was extracted

Figure 9. Excess material from the edges and mold shafts were trimmed from the extracted panel

E. WETSUIT CONSTRUCTION

Two of each type of composite panel were constructed in order to complete two wetsuits. A total of 13 panels per suit were fabricated. These include R/L shoulder, R/L upper back, R/L chest, Abdominal, R/L thigh, R/L shin, R/L forearm. Figure 10 shows several completed panels.

Figure 10. Several completed composite panels trimmed and labeled before being attached to the wetsuit

A custom-fitted wetsuit was created by Otter Bay Wetsuits in Monterey, CA. Once completed, composite panels were placed on the suit and outlined. Neoprene pockets were added around these outlines to enclose the full size of the panels and sealed with the pieces inside. The previous suit ran into issue at this phase, as pockets were added to be the size of the outlines themselves, forcing the author to further trim the composite pieces and reduce body coverage; this was corrected for the Mk. II suit. The final suit is shown in Figure 11.

Figure 11. Completed K-suit Mk. II with glass microsphere-based composite panels

THIS PAGE INTENTIONALLY LEFT BLANK

II. INVESTIGATION OF ACOUSTIC CHARACTERISTICS

While the Mk. II suit was completed and ready for dive testing to further investigate the improved thermal properties, the acoustic response of the composite materials needed to be investigated in a more controlled manner. Before physical tests were conducted, however, a basic theoretical prediction for the material performance was derived.

A. ACOUSTIC THEORY

Basic laws govern the reflection and transmission of sound transitioning between mediums. The reflection and transmission coefficients of the resultant sound waves are derived from the acoustic boundary conditions. In this case, however, the transmission of the sound is not incident on a single boundary, but a layer. One approach is to simply model this as transmission though a fluid layer. Neglecting the thin neoprene layer surrounding the panel for now, normal incidence on the three-medium layer is depicted by Figure 12. Media impedances are given as z_n and pressures are given as p_i, p_r, p_t for incidence, reflection, and transmission, respectively. L denotes the thickness of the central layer.

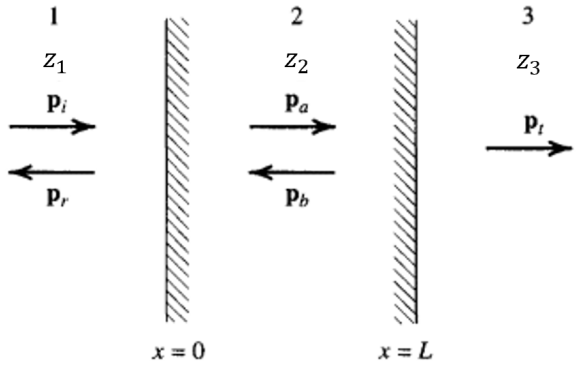

Figure 12. Transmission of normal incidence sound signal on a fluid layer. Adapted from [7].

Using a general expression for the incident signal [7], the waveform in the first medium can be expressed as

$$p_i = P_i e^{j(\omega t - k_1 x)}, \tag{3}$$

where the wavenumber is given as $k = \frac{2\pi}{\lambda}$ and $\lambda = \frac{c}{f}$.

Continuity of the specific acoustic impedance yields the pressure reflection coefficient and the intensity transmission coefficients [7]:

$$\boldsymbol{R} = \frac{\left(1-\frac{z_1}{z_3}\right)cosk_2L + j\left(\frac{z_2}{z_3}-\frac{z_1}{z_2}\right)sink_2L}{\left(1+\frac{z_1}{z_3}\right)cosk_2L + j\left(\frac{z_2}{z_3}-\frac{z_1}{z_2}\right)sink_2L} \tag{4}$$

$$T_I = \frac{4}{2+\left(\frac{z_3}{z_1}+\frac{z_1}{z_3}\right)cos^2k_2L + \left(\frac{{z_2}^2}{z_1z_3}+\frac{z_1z_3}{{z_2}^2}\right)sin^2k_2L} \tag{5}$$

This can be further reduced if the first and third fluids are the same. In the case of this experiment, the density of the human body is roughly the same as the surrounding seawater, making this an acceptable approximation [7]:

$$T_I = \frac{1}{1+\frac{1}{4}\left(\frac{z_2}{z_1}-\frac{z_1}{z_2}\right)^2 sin^2k_2L} \tag{6}$$

Furthermore, if $z_2 \gg z_1$, or the impedance of the second medium is much larger than that of the first, the intensity transmission coefficient reduces further [7].

$$T_I = \frac{1}{1+\frac{1}{4}\left(\frac{z_2}{z_1}\right)^2 sin^2k_2L} \tag{7}$$

It should be noted that for solid panels in water, if

$$\frac{z_2}{z_1} sink_2L \ll 1, \tag{8}$$

it further reduces to $T_I \approx 1$.

For all instances of T_I, the corresponding pressure transmission coefficient is derived as

$$T_P = \sqrt{T_I}. \tag{9}$$

While the above expressions for transmission coefficients are derived for normal incidence only, transmission for oblique incidence can be considered along the same lines and will vary with the incidence angle of the sound wave.

As the expression for the transmission intensity is derived, the impedances of the individual fluids must be determined. As the central medium is not a homogenous fluid, but a suspension of bubble-like glass microspheres, the sound speed of propagation can be approximated using Wood's equation for a gas bubble-liquid mixture in equilibrium. Note that equilibrium is obtained when the mixture is homogenous, such that every volume in the mixture contains a similar distribution of bubbles. As the elastomer base is thoroughly mixed with the glass microspheres before setting, an approximate equilibrium is reached. Wood's sound speed of propagation is given as [8]:

$$c_w{}^2 = \frac{1}{\rho_m K_m}. \tag{10}$$

The compressibility and density of a two-component mixture is given as:

$$K_m = K_f + K_p = \frac{1-C_v}{\rho_f c_f{}^2} + \frac{C_v}{\rho_p c_p{}^2} \tag{11}$$

$$\rho_m = \rho_f(1 - C_v) + \rho_p C_v \tag{12}$$

where C_v is the volume fraction of bubbles within the mixture, c_f is the liquid sound speed (elastomer base), ρ_f is the liquid density, c_p is gas sound speed, and ρ_p is the gas density [8].

This compressibility only takes the liquid and gas quantities into consideration. It must be expanded to include a third term to represent the glass microspheres themselves:

$$K_m = \frac{1-C_{air}-C_{glass}}{B_{elast}} + \frac{C_{air}}{\rho_{air} c_{air}{}^2} + \frac{C_{glass}}{B_{glass}} \tag{13}$$

$$\rho_m = \rho_{elast}\left(1 - C_{air} - C_{glass}\right) + \rho_{air} C_{air} + \rho_{glass} C_{glass} \tag{14}$$

B. BASIC FREQUENCY RESPONSE MODELS

In order to use these equations, values for the parameters were tabulated (Table 3). For certain variables, approximates were made from known quantities and sources are noted. Unless otherwise stated, values are known quantities or were from the K1 microsphere product information.

Table 3. Tabulated values for approximation of sound speed

Quantity	Comparable Value
ρ_{elast}	1110 kg/m^3 [9]
ρ_{air}	1.21 kg/m^3 (@ 20 C)
ρ_{glass}	2440 kg/m^3
c_{air}	343 m/s (@ 20 C)
c_{glass}	5560m/s [10]
$c_{elastomer}$	960-1110 m/s [11]
B_{glass}	43 GPa [10]
B_{elast}	1.5 GPa [12]

Using a three-component model with silicone, glass, and air results in an average density of about 510 kg/m^3 and an estimated sound speed of propagation of 22 m/s. This value is extremely low and is not an accurate approximation. This is due to the fact that Wood's equation assumes the material components are at the same pressure, which is not the case with the air sealed within the glass microspheres. It should be noted that these values are not ideal for a sound absorber, as the density is much lower than water and features a slower sound speed of propagation. Referring to the condition presented in Equation 8, it would be hypothesized that no mitigation of transmitted intensity would be measured. This condition is seen below in Figure 13, where the left side of the inequality is plotted. With a thickness of ~ 1 cm, there is no mitigation expected across all frequencies.

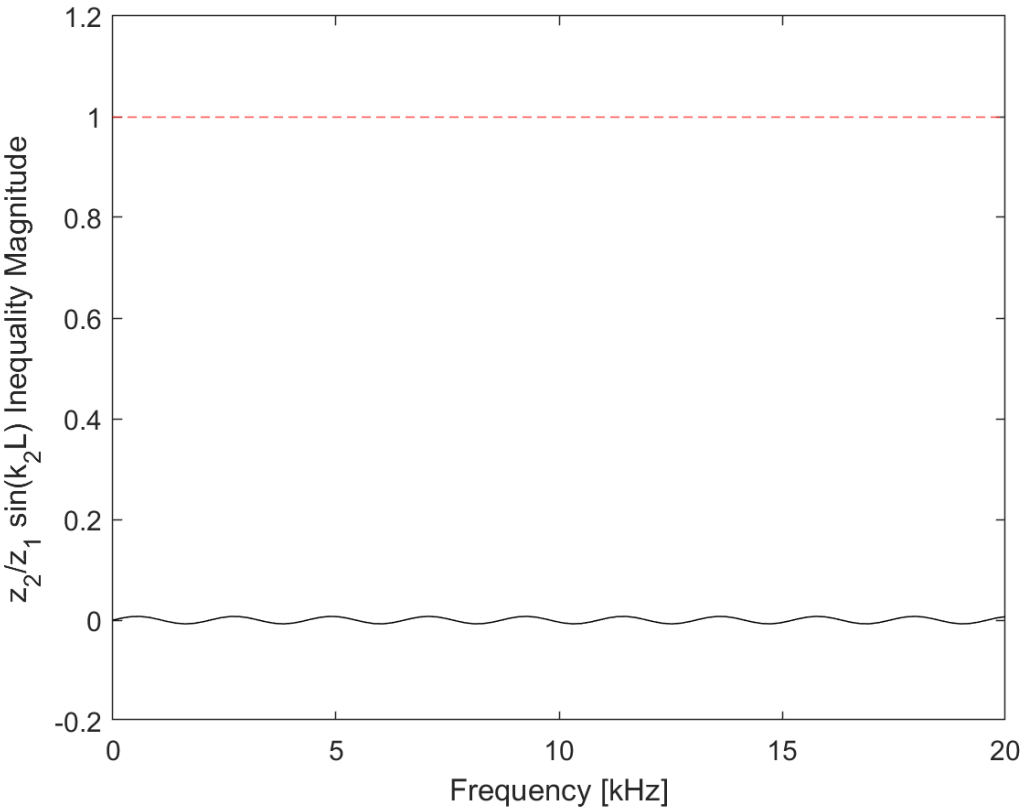

Figure 13. Plot of the left-hand cutoff inequality (black) for the 3-component approximation. Note that it never approaches a magnitude near 1 to satisfy the inequality

Another approach would be to model the panels as a two-component mixture of glass microspheres suspended in the silicone elastomer, neglecting the air within them. This results in an average density of about 1950 $\mathrm{kg/m^3}$ and estimated sound speed of 5870 m/s. A plot of the expected transmission curves for this two-component approximation is shown in Figure 14. Using this approximation, it would be expected for a reduction in transmitted intensity to occur beginning around 10 kHz.

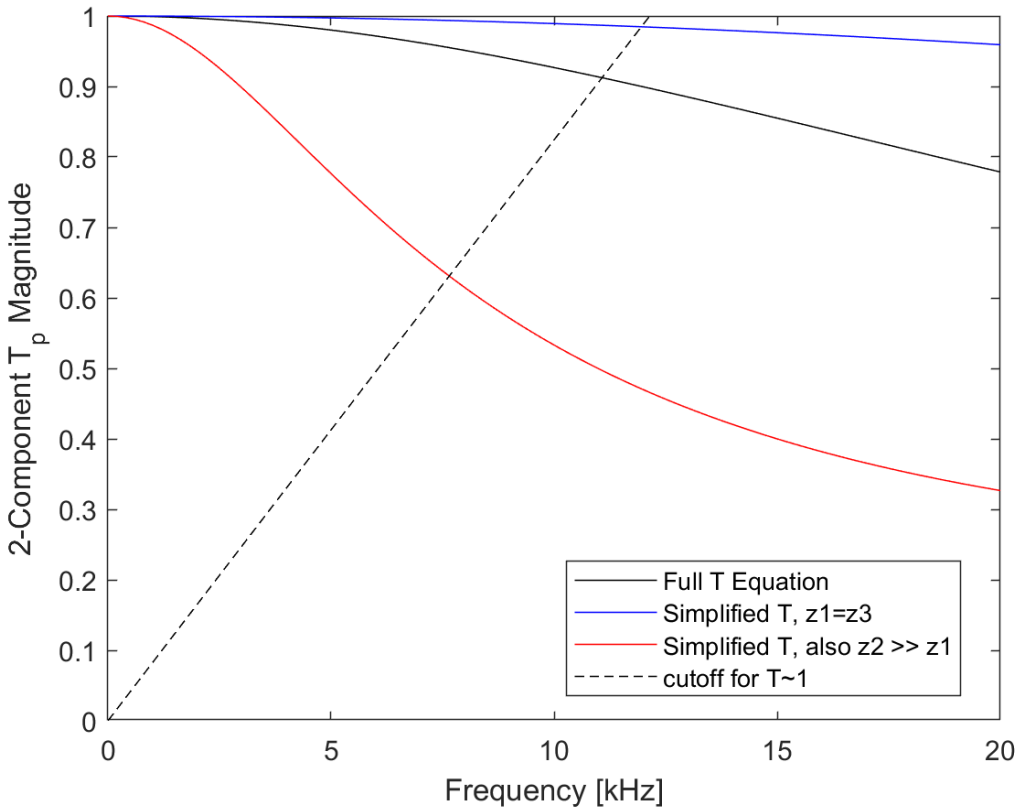

Figure 14. Estimated transmission curves for the two-component approximation using silicone elastomer and glass (neglecting air)

Finally, a third transmission curve was created to model the panels simply as solid glass. In this case, the sound speed of glass is known to be about 5560 m/s with a density of 2440 $\mathrm{kg/m^3}$. This model is plotted in Figure 15, showing the most drastic decrease in transmitted intensity out of the three models.

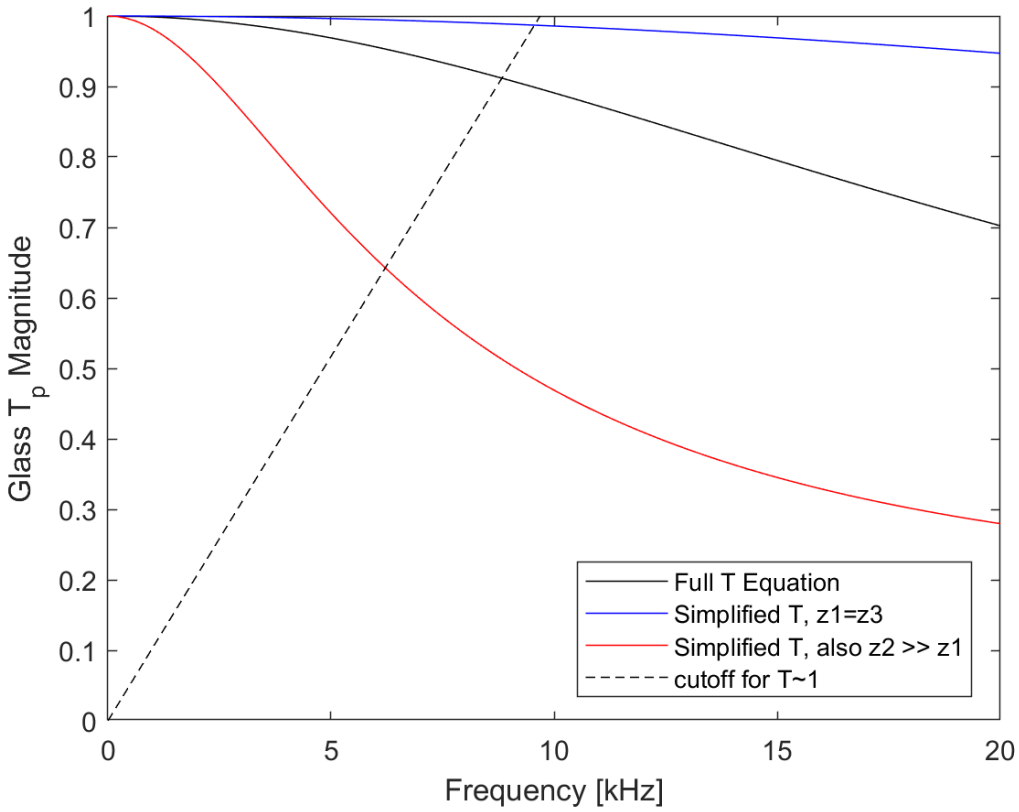

Figure 15. Estimated transmission curves for simplistic glass model (neglecting air and silicone elastomer base)

It should be noted that the simplified transmission equation for $z_2 \gg z_1$ is not applicable for the constructed panel, as it cannot accurately be modelled as a solid glass panel. What these transmission curves do show, however, is that any reduction in transmission that occurs will take place after about 10 kHz. For a 1 cm test panel, this is to be expected; a small signal wavelength relative to this thickness is necessary to have any significant impact on reducing transmission. A frequency range from 5 to 20 kHz corresponds to wavelengths varying from approximately 30 to 7.5 cm, which are fairly large compared to this material thickness.

THIS PAGE INTENTIONALLY LEFT BLANK

III. EXPERIMENTAL SETUP

Composite pucks of the same composition as the wetsuit panels were used to test the acoustic frequency response of the material. Several pucks, with slight variation in K1 microsphere content, were used to investigate the relationship to material density. The first puck labelled "O5," was created with a microsphere content of 18.5% by volume with an average material density of 854 kg/m^3. A second puck, "O10," was created to be 52.6% microspheres by volume with an average density of 549 kg/m^3 (Figure 16). All material pucks were created with a diameter of 13.5 cm.

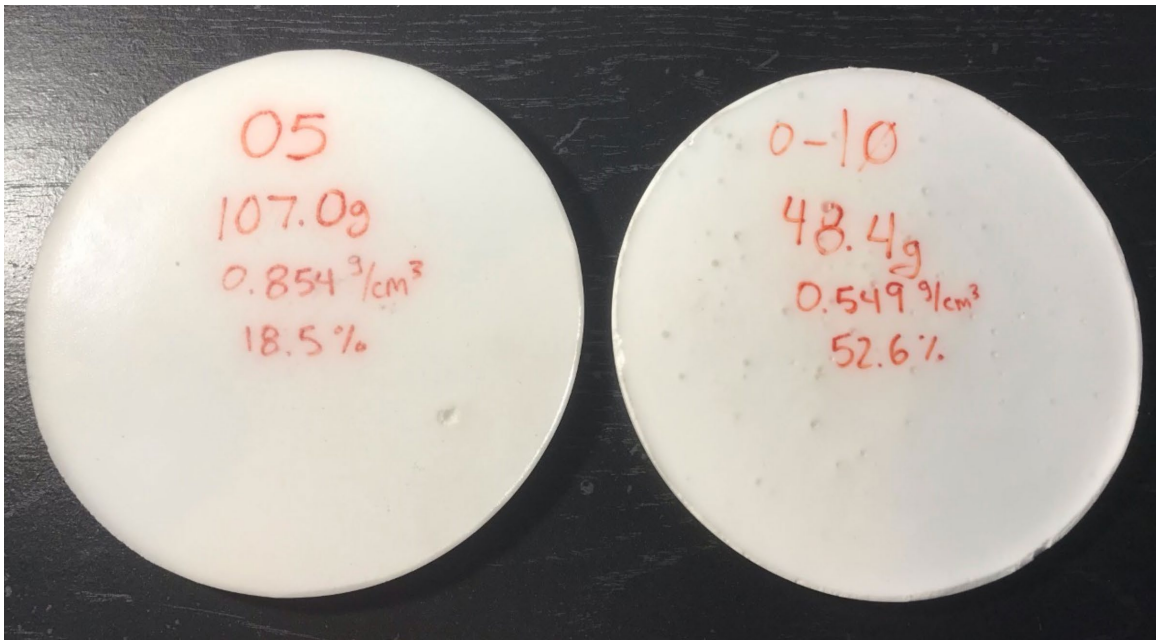

Figure 16. O5 and O10 composite pucks constructed with glass microspheres

The test arrangement was based around a University Sound Model UW-30 underwater speaker to generate a chirp incident signal. This speaker, mounted 1m underwater in a tank with anechoic lining, was driven by an HP Power Amplifier (467A) with a 5x voltage gain from a 1V function generator. A Brüel & Kjær (B&K) 8103 hydrophone, placed 1 m underwater and approximately 1.5 m from the speaker (Figure

17), was used to record the pressure generated by the speaker's output. This hydrophone was placed directly behind the testing material and was in contact with the puck and/or neoprene for each test. This hydrophone was fed into an SRS Model SR560 Low Noise Preamplifier to increase the signal by a factor of 10. This also utilized a low pass filter at 30 kHz and a high pass filter at 100 Hz to reduce noise. Both the amplified hydrophone and speaker signals were input to a Stanford Research Systems (SRS) Model SR785 2-Channel Dynamic Signal Analyzer to perform a 100 Hz to 20 kHz sweep. The results of this were recorded via Tektronix MD03014 Mixed Domain Oscilloscope.

Figure 17. Hydrophone and composite puck arrangement behind neoprene material (held out of tank for visualization)

An additional frame was used to hold a 7 mm thick neoprene square, with a side length of about 30 cm, to log the neoprene's response as well. A gated FFT sweep (Figure 18) was conducted first to ensure no sound reflections would be present during recording. No echoes appeared during the testing, indicating that reflections were negligible.

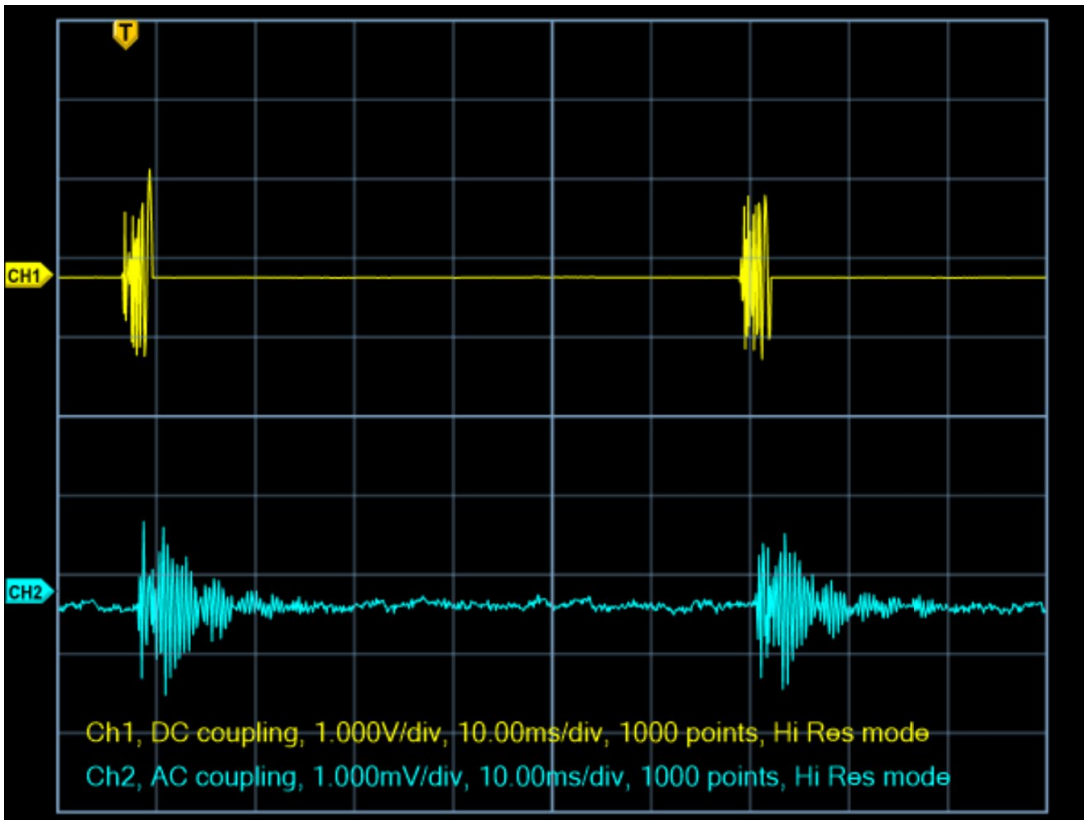

Figure 18. A gated FFT sweep was conducted to verify that no sound echoes/reflections were present. Ch.1 (Yellow) shows the speaker chirp, while Ch.2 (Blue) is the hydrophone recording

IV. RESULTS AND ANALYSIS

A. FREQUENCY RESPONSE

Sweeps were conducted for several arrangements, with the first being only the hydrophone. This recording was used as the baseline to compare to the subsequent measurements. The next setup saw the neoprene panels affixed to the frame and suspended 1m underwater. The hydrophone was attached to a ring stand and suspended into the tank behind the neoprene test material. This was repeated twice with the addition of the O5 and O10 pucks placed between the neoprene and the hydrophone. An additional two tests were conducted to record the response of the O5 and O10 pucks individually without the neoprene. Figure 19 shows the raw data recording converted from captured dB re V/µPa units to pressure units of Pa.

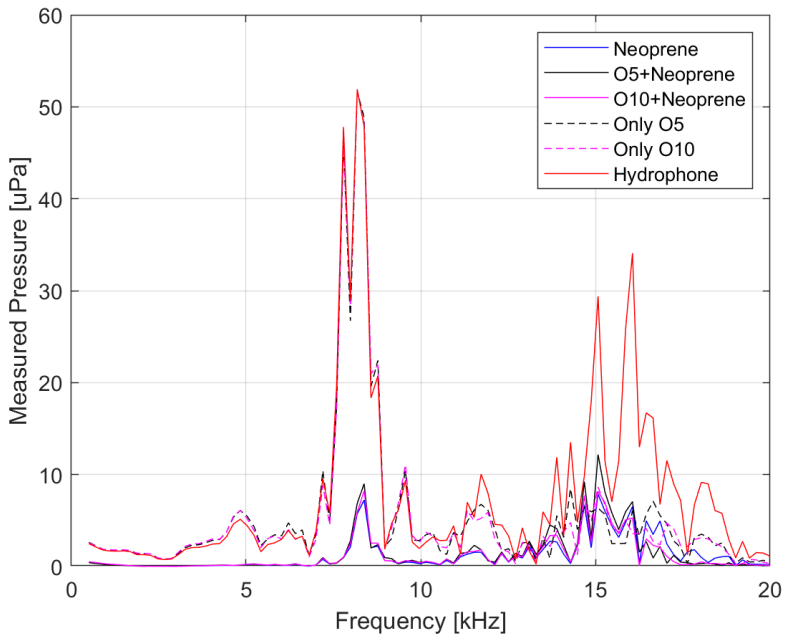

Figure 19. Raw captured data showing frequency response for the tested materials in units of pressure (converted from captured dB re V/µPa)

From these data captures, it can be seen that the hydrophone does not have a uniform frequency response, making it more difficult to visualize trends in sound pressure reduction as frequency increase. As such, this data will be analyzed in terms of the ratio between the pressure measured behind the material shielding and the hydrophone baseline. It should also be noted that certain frequency ranges show an increase in recorded pressure for various materials.

B. PRESSURE REDUCTION

This data was translated into the ratio between the measured acoustic pressure behind the material shielding to the hydrophone baseline pressure; Figure 20 shows this unitless ratio for all materials. As seen in this response curve, certain materials, namely the pucks themselves, resulted in a higher measured acoustic pressure. The neoprene and combination of composite pucks and neoprene generally reduced the measured pressure with exception of a noticeable spike around 13 kHz for the O5 and O10 combinations. This increase for the O5 and O10 pucks, while not originally expected, can possibly be explained by diffraction around the sides of the pucks themselves. Due to the relatively small diameter of these materials, lower frequencies (greater wavelengths) may experience some constructive interference from the bending sound waves, resulting in a measurable increase in pressure.

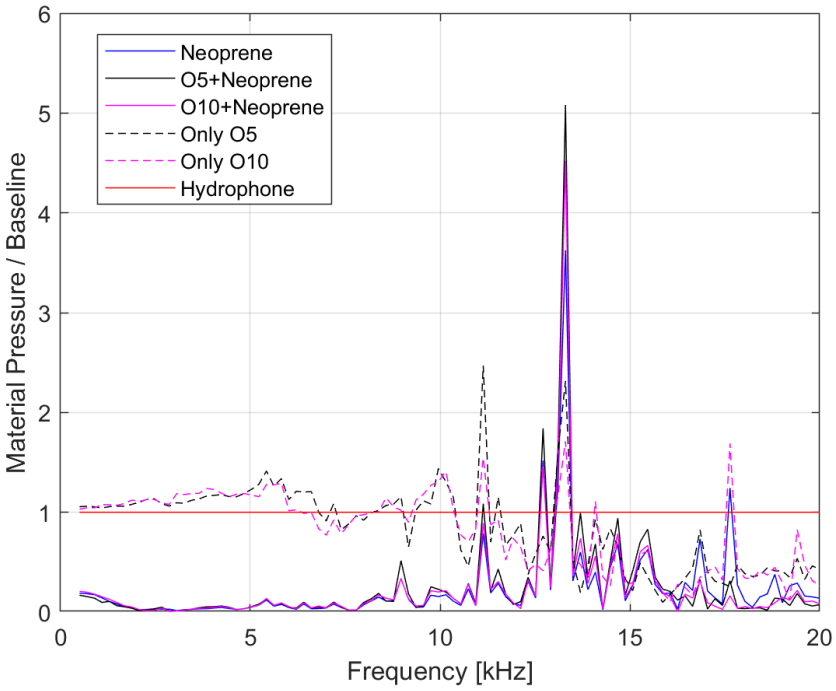

Figure 20. Ratio of measured pressure behind material shielding and hydrophone baseline

The same ratios for the individual O5 and O10 pucks were also plotted separately to visualize trends more clearly in the data (Figure 21). As anticipated in the theoretical predictions, sound absorption within the pucks does not occur until around 10 kHz and generally increases from this frequency; this is likely primarily determined by the thickness of the composite materials. Again, several prominent increases in measured pressure are recorded at certain frequencies for all materials, including neoprene.

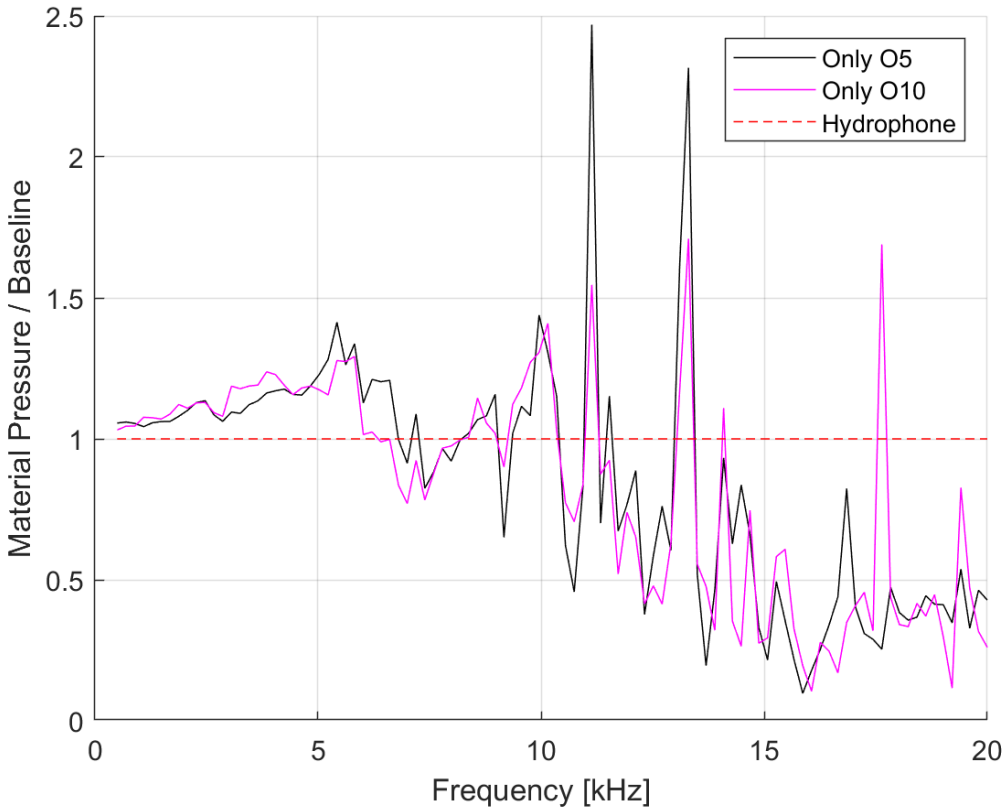

Figure 21. Ratio of measured pressure behind O5 and O10 pucks and hydrophone baseline

This pressure reduction was also plotted in units of dB (Figure 22). A negative value refers to a ratio of less than one and indicates a reduction in pressure from the baseline. Note that this dB representation is not an SPL value, as it is not referenced to an acoustic pressure. When placed in combination with neoprene, the O5 and O10 pucks are seen to have a response similar to neoprene as expected, but do not contribute any significant pressure reduction themselves until higher frequencies.

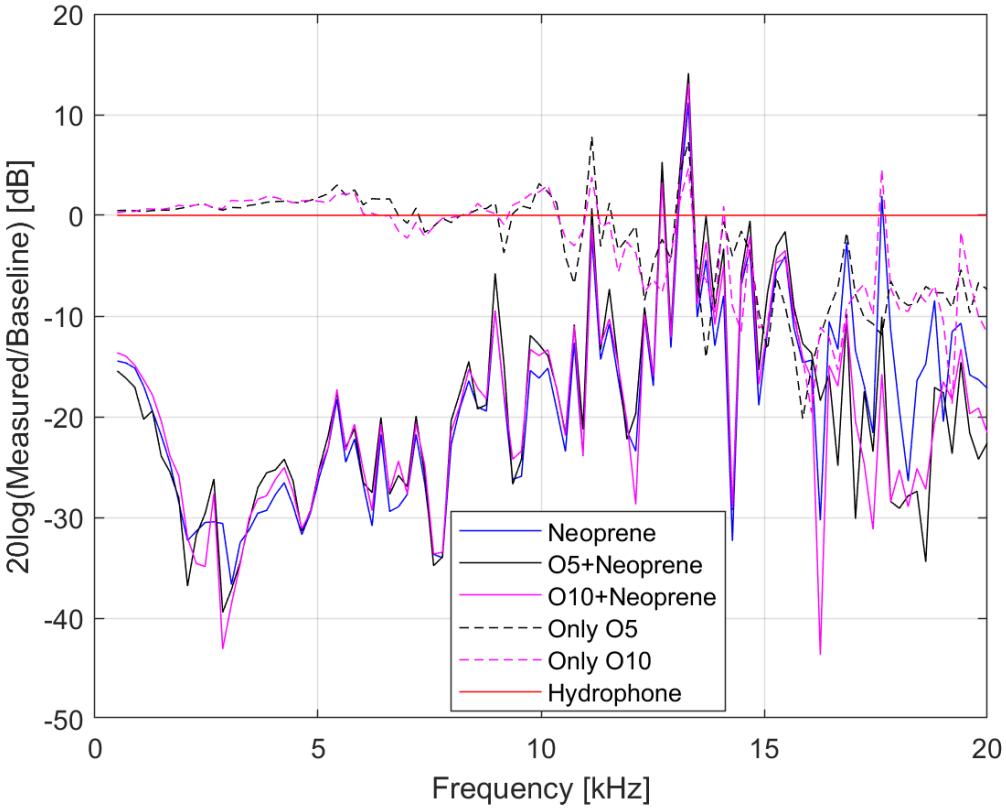

Figure 22. Ratio between measured material pressure and hydrophone baseline in dB

This ratio is again plotted (Figure 23) with only the composite O5 and O10 pucks to discern the response more clearly. Past a frequency of 10 kHz, the reduction is more significant and can be seen to improve with frequency.

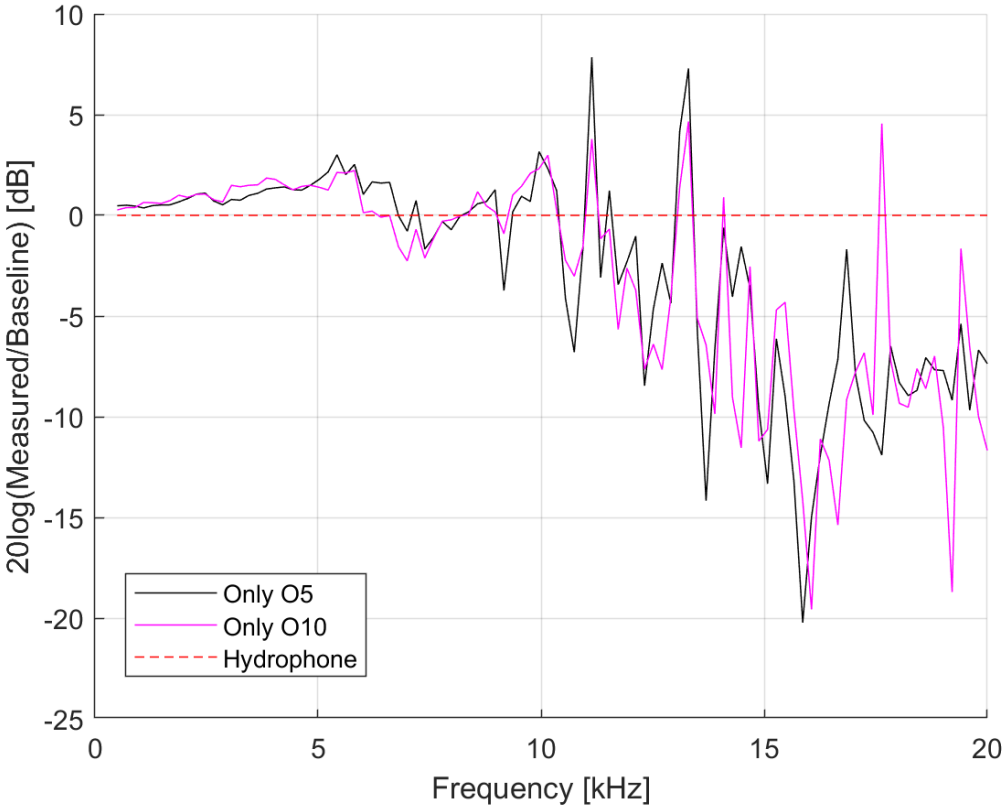

Figure 23. Ratio between measured O5 and O10 pressure and hydrophone baseline in dB

C. TRANSMISSION

The reduction in pressure from the hydrophone baseline in units of pressure (Pa) was then used to model the pressure transmission coefficient for each material. With this calculated, the results could be compared to the initial material predictions. These values for the pressure transmission coefficient are presented in figures 24 and 25.

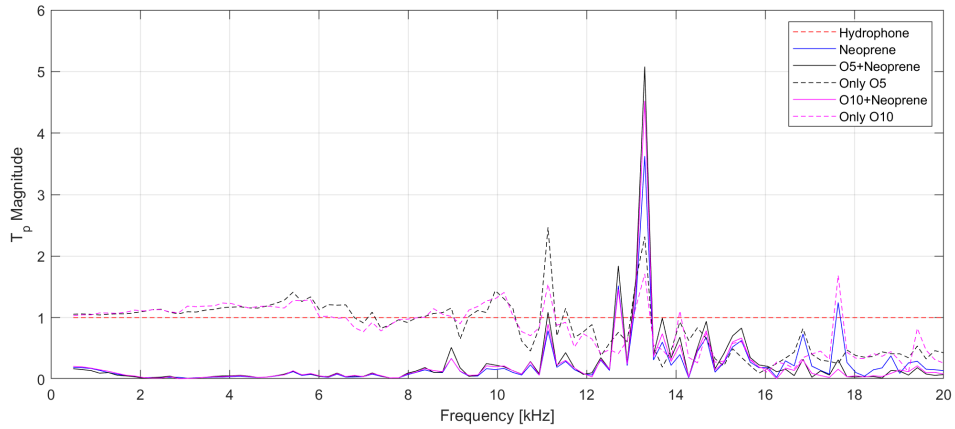

Figure 24. Pressure transmission coefficients for all tested materials relative to hydrophone baseline

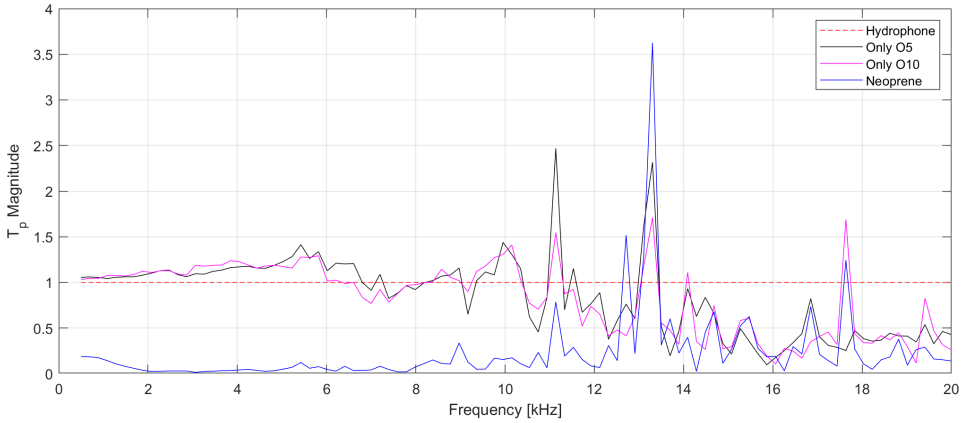

Figure 25. Pressure transmission coefficients for composite material pucks relative to hydrophone baseline

D. CERAMIC MICROSPHERES

Additional pucks were created using 3M ceramic microspheres to compare the obtained frequency response at similar compositions to the glass microsphere pucks previously explored. These pucks were constructed with the same methodology presented and similar ratios of 20% and 50% ceramic microspheres by volume (comparable to 18.5% "O5" and 52.6% "O10" composite samples). The same tank and equipment arrangement was used. The acoustic response of this second material was investigated as it is likely to be used for further thermal testing in the near future. The ceramic microsphere samples are

denoted as “C20” and “C50” for the 20% and 50% compositions, respectively. The resultant frequency response is plotted in Figure 26.

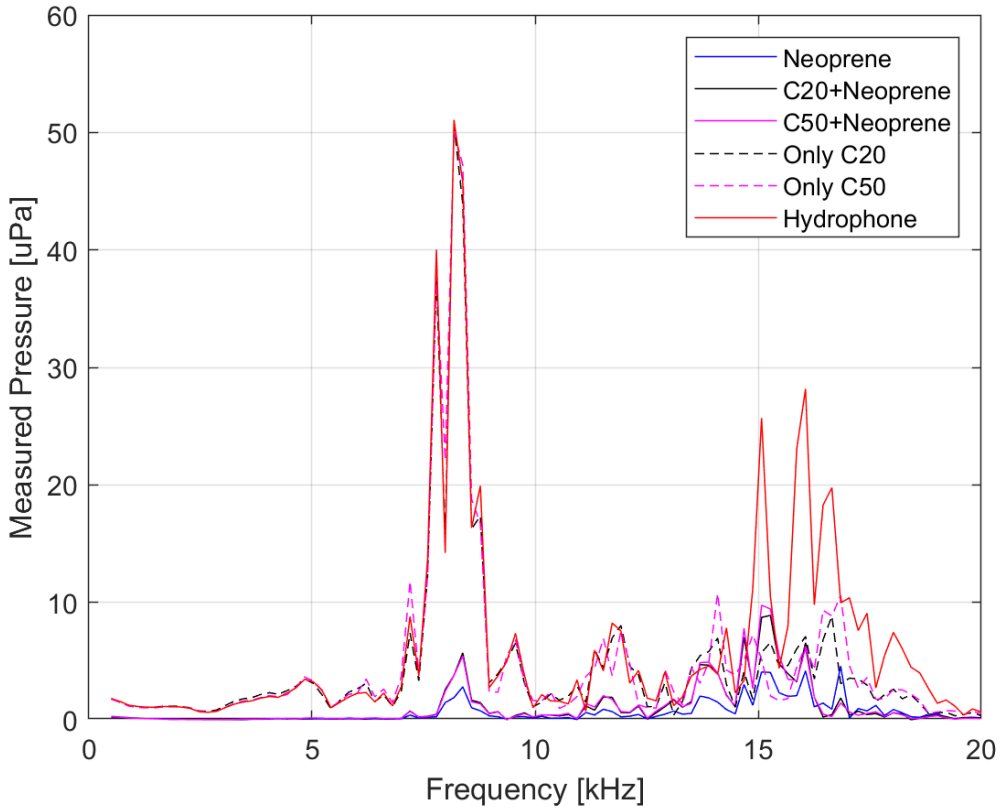

Figure 26. Ceramic frequency response of C20 and C50 material pucks

This data was again translated into a ratio between the measured shielded pressure and the hydrophone baseline (Figure 27). From this response curve, the neoprene and C20 and C50 pucks (in combination with the neoprene) have a similar frequency response.

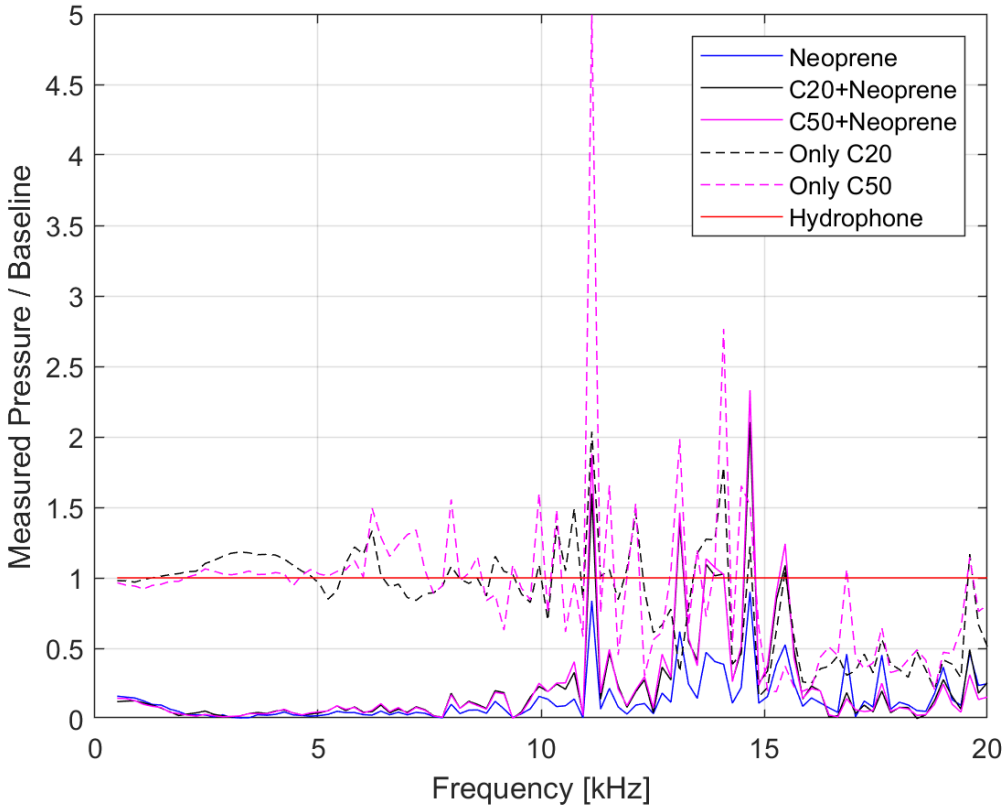

Figure 27. Ratio of measured pressure behind ceramic material shielding and hydrophone baseline

As with the composite panels, the individual ratios of the C20 and C50 pucks are plotted without the addition of neoprene shielding (Figure 28). Once again, it can be seen that the thickness of the material does not allow for any noticeable pressure reduction at lower frequencies. Interestingly, the C50 puck produces an extremely high peak around 11 kHz.

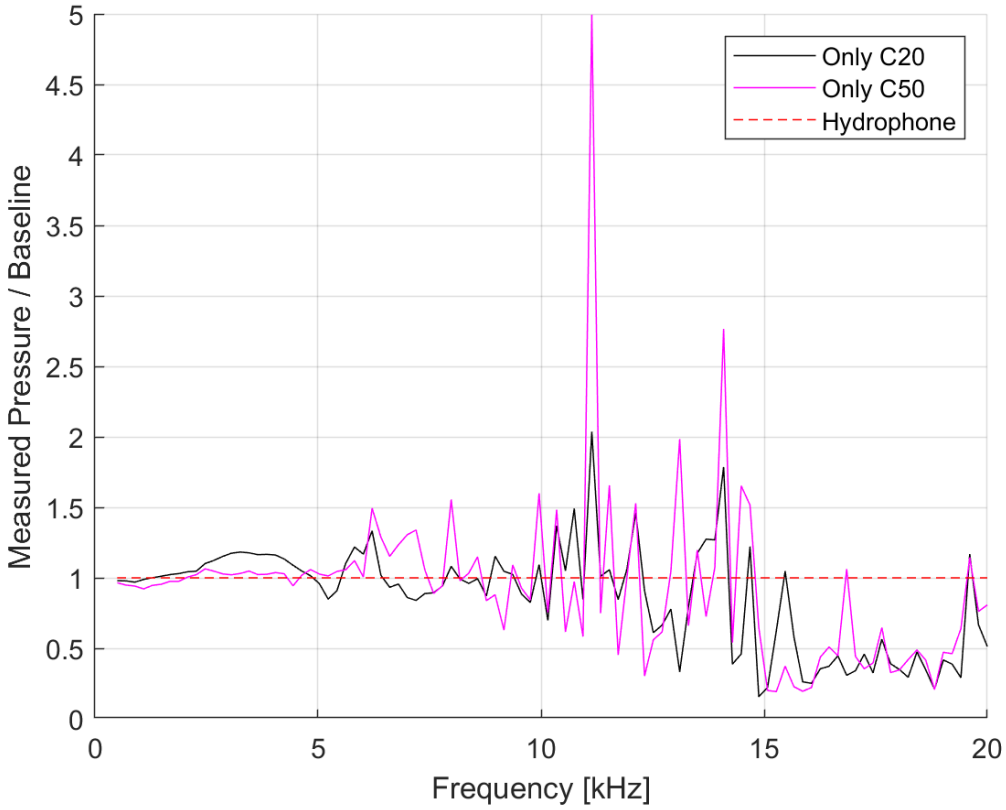

Figure 28. Ratio of measured pressure behind C20 and C50 pucks and hydrophone baseline

These results are again converted to dB values and are plotted in Figure 29. Note that negative values continue to demonstrate a reduction in pressure whereas positive values denote an increase in measured pressure.

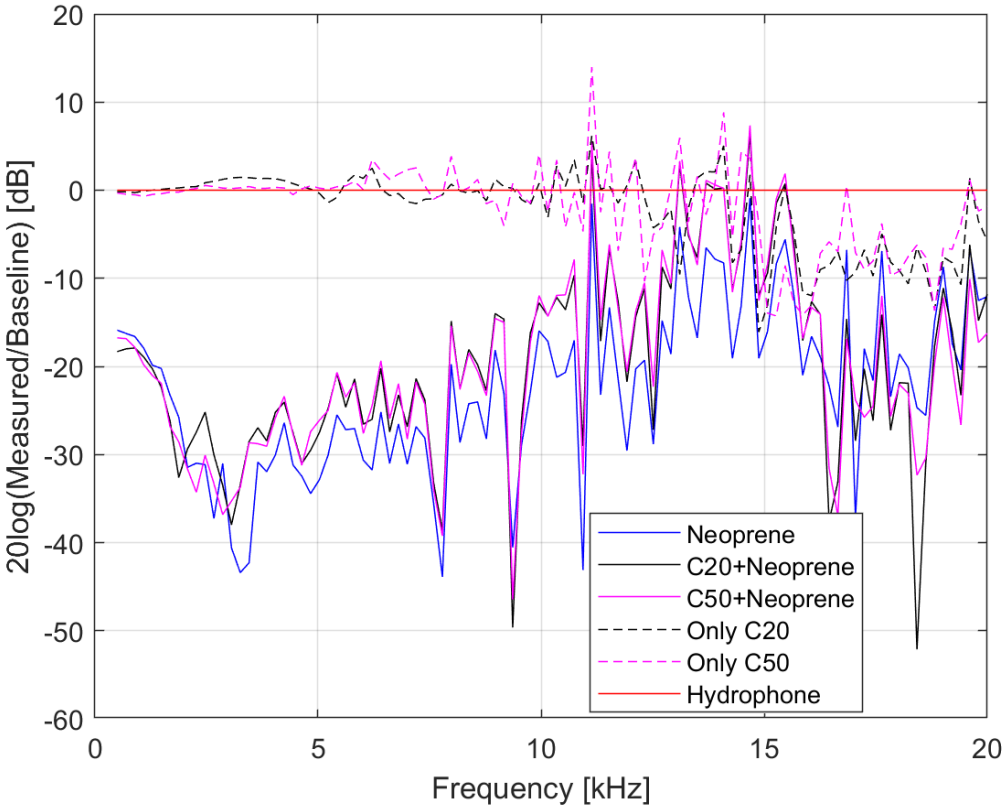

Figure 29. Ratio between measured ceramic material pressure and hydrophone baseline in dB

This data is plotted once more for the individual ratios of the C20 and C50 material pucks. Figure 30 shows a similar response as compared to the original glass composite material. While there appears to be similar attenuation at lower frequencies, there is a high degree of pressure reduction variability until about 13 kHz, where it begins to perform similarly to the glass composite.

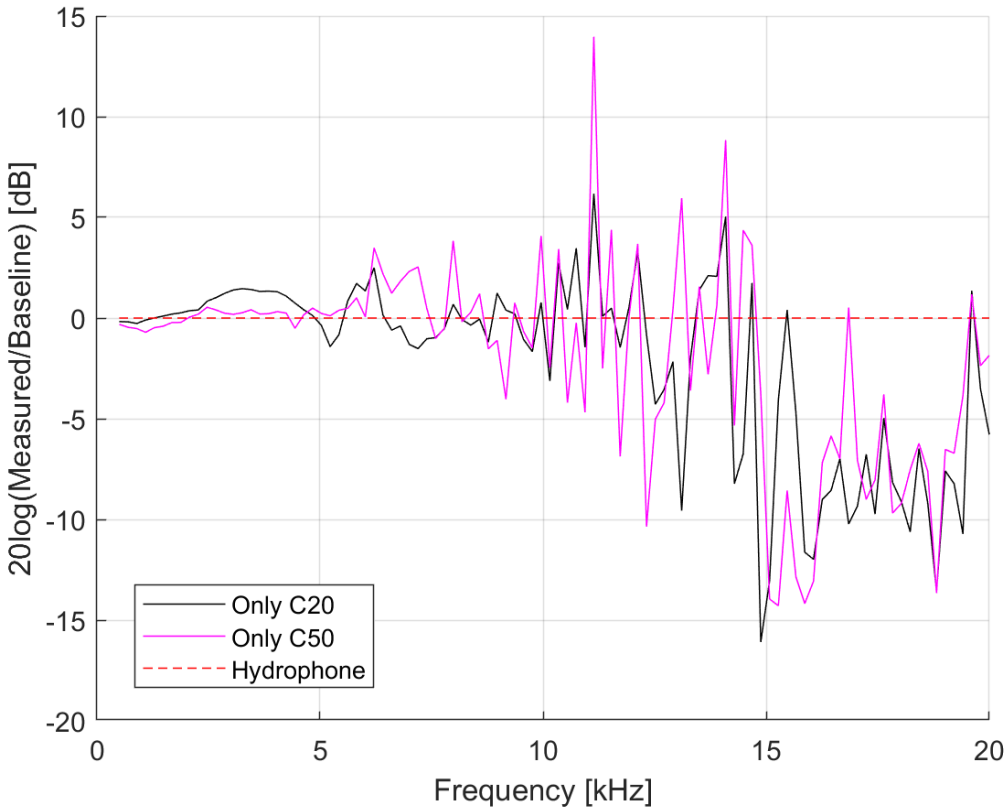

Figure 30. Ratio between measured C20 and C50 pressure and hydrophone baseline in dB

Finally, figures 31 and 32 show the plotted pressure transmission coefficients for all materials and the individual ceramic puck responses, respectively. Compared to the glass composite material, the ceramic transmission response is much more variable. A response comparable to the composites is only evident again after about 13 kHz.

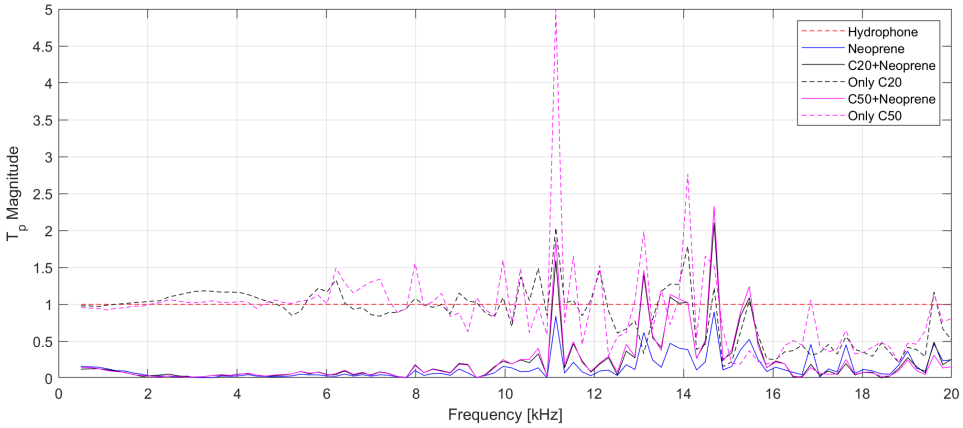

Figure 31. Pressure transmission coefficients for all tested ceramic materials relative to hydrophone baseline

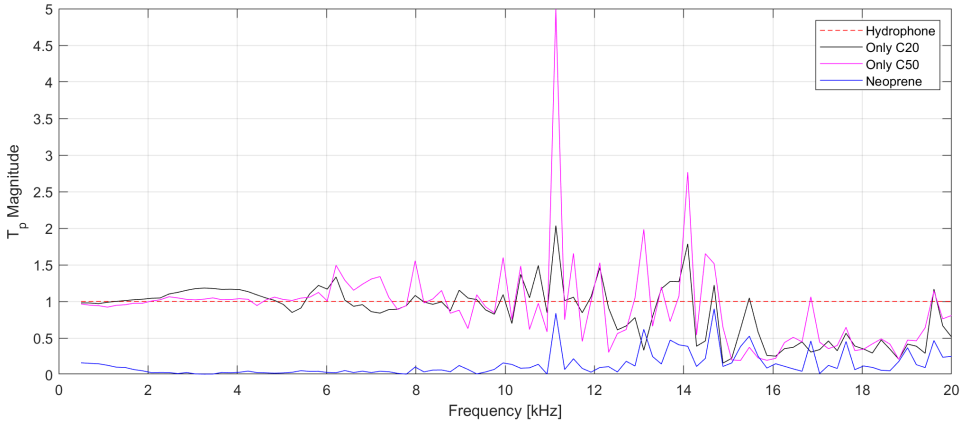

Figure 32. Pressure transmission coefficients for ceramic material pucks relative to hydrophone baseline

E. MATERIAL COMPARISON

The measured sound pressure reduction of the individual composite materials indicates a level of successful soundproofing past a frequency of about 10 kHz as expected. Recorded spikes may be indicative of resonance within the neoprene, as composite and ceramic spikes correspond to similar ones measured while testing neoprene. The combination of composite and ceramic materials and neoprene further reduce the sound pressure as compared to the individual neoprene recording, but not by a significant amount. Calculated pressure transmission coefficients also indicate a trend for improved pressure

reduction as frequency increases for both materials. This confirms the basic modelling predictions and can be explained by the decreasing signal wavelength.

The measured response of the materials both suggest little to no attenuation at lower frequencies. At the higher frequencies tested, the materials respond in a similar manner, exhibiting peaks and nulls at the same frequencies. This behavior may suggest that the response is more closely tied to the silicone elastomer itself rather than the embedded microspheres. As such, the elastomer base should be tested in the future and the results compared. Higher frequencies should also be tested with an additional sound source to understand the full spectrum response. Additionally, more in-depth modelling would be useful in accurately predicting the material response. Larger material pucks should be tested to reduce any effects of sound diffraction that may be causing the frequency-dependent variations within the pressure recordings.

V. CONCLUSION

The K-suit Mk II was completed, and the material's SPL reduction capabilities were tested. Both the glass microsphere-based composite panels and additional ceramic microsphere panels yielded a reduction in measured SPL when compared to the baseline hydrophone signal. These materials did not, however, surpass the sound-proofing capabilities presented by neoprene alone and failed to produce any attenuation at lower frequencies. While these results were predicted, the material responses suggest that a combined usage of neoprene and composite material will result in a noticeable SPL reduction at higher frequencies while also affording the thermal protection provided by the additional panels. Preliminary results also suggest that the SPL reduction will increase at higher frequencies due to limitations presented by material thickness.

The addition of these panels will allow divers to utilize a thinner neoprene wetsuit while retaining the thermal protection properties afforded by a thicker suit. Specific placement of material may also act to increase diver sound tolerance in terms of timed exposure and intensity level while operating near underwater sound sources. Such an increase would allow for a change in Navy operating procedure and combat diving capabilities. Although the composite and ceramic materials were outperformed by neoprene, the addition of such panels may present a non-compressible sound-proofing solution when paired with neoprene and used at greater pressures. Additional testing at higher pressures could confirm this hypothesis.

THIS PAGE INTENTIONALLY LEFT BLANK

LIST OF REFERENCES

[1] S. L. Martin, "Building and testing an incompressible thermally insulating cold temperature diving wetsuit," M.S. thesis, Dept. of Applied Physics, NPS, Monterey, CA, USA, 2020. [Online]. Available: http://hdl.handle.net/10945/66103

[2] C. Brummet and N. R. Raju, "An investigation into the use of neoprene (a red listed material) for soundproofing," University of British Columbia, Nov. 2010. [Online]. Available: https://open.library.ubc.ca/cIRcle/collections/undergraduateresearch/18861/items/1.0108313

[3] *U.S. Navy Diving Manual*, SS521-AG-PRO-010, NAVSEA, Washington, DC, USA, 2016. [Online]. Available: https://www.navsea.navy.mil/Portals/103/Documents/SUPSALV/Diving/US%20DIVING%20MANUAL_REV7.pdf?ver=2017-01-11-102354-393

[4] S. Parvin, "Limits for underwater noise exposure of human divers and swimmers," presented at the Subacoustech, [Online]. Available: http://resource.npl.co.uk/docs/science_technology/acoustics/clubs_groups/13oct05_seminar/parvin_subacoustech.pdf

[5] Applied Research Laboratories, University of Texas at Austin, "Non-lethal swimmer neutralization study," San Diego, CA, USA, Rep. 3138, 2002. [Online]. Available: https://web.archive.org/web/20060427061028/http://www.spawar.navy.mil/sti/publications/pubs/td/3138/td3138cond.pdf

[6] A. P. Demers, "Depth independent thermal insulation for diving suits," M.S. thesis, Dept. of Applied Physics, NPS, Monterey, CA, USA, 2020. [Online]. Available: http://hdl.handle.net/10945/65500

[7] L. E. Kinsler, A. R. Frey, A. B. Coppens, and J. V. Sanders, *Fundamentals of Acoustics*, 4th ed. Hoboken, NJ, USA, John Wiley & Sons, Inc., 2000.

[8] S. Temkin, "Sound Propagation in Bubbly Liquids: A Review," Naval Research Laboratory, Washington, DC, Memorandum Report, May 1989. [Online]. Available: https://apps.dtic.mil/dtic/tr/fulltext/u2/a207377.pdf

[9] Dow Corning, *Sylgard(R) 184 silicon elastomer kit,* 802554-00007, 2014. [Online]. Available: https://www.wpiinc.com/pub/media/wysiwyg/pdf/sylgard-184-base-msds.pdf

[10] B. Henneberry, "All about soda lime glass - composition and properties," Thomasnet. Accessed May 1, 2021. [Online]. Available: https://www.thomasnet.com/articles/plant-facility-equipment/soda-lime-glass/

[11] D. L. Folds, “Speed of sound and transmission loss in silicone rubbers at ultrasonic frequencies,” *The Journal of the Acoustical Society of America*, vol. 56, pp. 1295–1296, 1974.

[12] AZO Materials, “Silicone Rubber.” Accessed May 1, 2021. [Online]. Available: https://www.azom.com/properties.aspx?ArticleID=920

INITIAL DISTRIBUTION LIST

1. Defense Technical Information Center
   Ft. Belvoir, Virginia

2. Dudley Knox Library
   Naval Postgraduate School
   Monterey, California